Available online at www.sciencedirect.com
ScienceDirect
Trans. Nonferrous Met. Soc. China 24(2014) 2244−2250
Transactions of Nonferrous Metals Society of China
www.tnmsc.cn

Effects of Al−Ti−B−RE grain refiner on microstructure and mechanical properties of Al−7.0Si−0.55Mg alloy

Xue-jiao WANG[1], Cong XU[1], Arfan MUHAMMAD[1], Shuji HANADA[2], Hiroshi YAMAGATA[3], Wen-hong WANG[4], Chao-li MA[1]

1. Key Laboratory of Aerospace Advanced Materials and Performance of Ministry of Education, School of Materials Science and Engineering, Beihang University, Beijing 100191, China;
2. Institute for Materials Research, Tohoku University, Sendai 980-8577, Japan;
3. Center for Advanced Die Engineering and Technology, Gifu University, 1-1 Yanagido, Gifu City, Gifu 501-1193, Japan;
4. Hebei Sitong New Metal Material Co., Ltd., Baoding 071105, China

Received 17 October 2013; accepted 30 April 2014

Abstract: To investigate the effects of Al−Ti−B−RE grain refiner on microstructure and mechanical properties of Al−7.0Si−0.55Mg (A357) alloy, some novel Al−7.0Si−0.55Mg alloys added with different amount of Al−5Ti−1B−RE grain refiner with different RE composition were prepared by vacuum-melting. The microstructure and fracture behavior of the Al−7.0Si−0.55Mg alloys with the grain refiners were observed by X-ray diffraction (XRD), optical microscopy (OM), scanning electron microscopy (SEM), and the mechanical properties of the alloys were tested in mechanical testing machine at room temperature. The observation of Al−Ti−B−RE morphology and internal structure of the particles reveals that it exhibits a $TiAl_3/Ti_2Al_{20}RE$ core-shell structure via heterogeneous TiB_2 nuclei. The tensile strength of Al−7.0Si−0.55Mg alloys with Al−5Ti−1B−3.0RE grain refiner reaches the peak value at the same addition (0.2%) of grain refiner.

Key words: A357 alloy; Al−5Ti−1B grain refiner; rare earth; fracture; refining effect; tensile strength

1 Introduction

Grain refinement by inoculation involves addition of particles which can act as substrates for heterogeneous nucleation. Grain refinement of Al and its alloys by the addition of Al−5Ti−1B master alloys to liquid melt prior to casting is a common practice in order to achieve a fine equiaxed grained microstructure in a casting which otherwise solidifies usually with coarse columnar grain structure. Hypoeutectic cast A1−7.0Si−0.55Mg alloy has been widely used for several applications, including automotive parts, aircraft structures, and engineer controls, owing to its excellent cast ability, weld ability, corrosion resistance, and good mechanical properties [1]. It is well known that an equiaxed grain structure ensures uniform mechanical properties, reduced hot tearing, improved feeding to eliminate shrinkage porosity, distribution of second phases and microporosities on a fine scale as well as improved machinability in castings. Based on the relationship between microstructures and properties, adding grain refining agents into the aluminum alloy is one of the effective ways to decrease the grain size and improve its mechanical properties. The addition of the grain refiner can promote the equiaxed grain's formation and impede the dendritic crystal nucleation and growth. The addition of a small amount of grain refiner to the aluminium melt can promote the formation of equiaxed grains, which improves the mechanical properties and reduces the ingot cracking. Currently, the most widely used grain refiner is Al−Ti−B grain refiner [2−7]. ARNBERG et al [8] have made detailed study on the influence morphologies of $TiAl_3$ particles on the grain refining behaviour and they concluded that flake and petal-like $TiAl_3$ particles will make the master alloy as low acting and long-lasting one,

Foundation item: Project (2012CB619503) supported by the Natioanl Basic Research Program of China; Project (2013AA031001) supported by the National High-tech Research and Development Program of China; Project (2012DFA50630) supported by the International Science & Technology Cooperation Program of China
Corresponding author: Chao-li MA; Tel: +86-10-82339772; E-mail: clma2001@gmail.com
DOI: 10.1016/S1003-6326(14)63340-9

while compact blocky particles make it a fast acting and early fading one. MOHANTY et al [5,9] observed a $TiAl_3$ layer around TiB_2 particles in Al−Ti−B master alloys. However, YU and LIU [10] considered that it was not $TiAl_3$ but a Ti-rich zone around the TiB_2 particle in Al−Ti−B master alloys. However, there are some problems with Al−Ti−B alloy, such as agglomeration of the borides, blockage of filters, defects during subsequent forming operations, and in some alloys Cr, Zr, Li and Si are contained as alloying elements which make them respond poorly to grain refinement by Al−5Ti−1B master alloy [11−13], which is usually termed as poisoning effect. It is generally believed that the poisoning elements interact with the grain refining constituents of the Al−Ti−B master alloys (Al_3Ti and TiB_2) and make them ineffective or less effective [14−21]. As a resolution, the rare earth elements could be added to decrease or even eliminate the drawbacks of the Al−Ti−B grain refiner, and make the refining agent to obtain more favorable performance. Although much work has been done to establish the grain refining mechanism and the influence of various parameters such as Ti content, Ti/B ratio, contact time and temperature on the grain refining efficiency, there are less researches on grain refinement effect of RE content in the references.

The aim of the current study was to determine the Al−5Ti−1B−RE grain refiners to provide effective grain refinement on A1−7.0Si−0.55Mg alloy. The effects of the level of the grain refiner were also analyzed in detail.

2 Experimental

A series of laboratory Al−5Ti−1B−RE grain-refining tests were conducted using a commercial Al−7.0Si−0.55Mg alloy (A357) supplied by Hebei Sitong New Metal Material Co., Ltd., and the composition of A357 is listed in Table 1. A wide range of candidate grain refiner materials were selected, as listed in Table 2. The melting operation was performed in JZ-IMT WZG-2 vacuum melting furnace. Once the melt reached 750 °C, it was degassed for 10 min with argon gas at a flow rate of 1.5 L/min. The grain refiners were added at three additions levels: 0.2%, 0.3%, 0.4% (mass fraction) of the mass of A357. Each refiner addition level had five separate melts and five castings. This procedure provided an indication of the reproducibility of the results. The desired amount of grain refiner was added by submerging it into the melt until fully molten. The contact time for the grain refiner was nominal 10 min, during which the furnace was kept switched on; both to maintain temperature and to mix the grain refiner. The melt temperature was monitored to ensure the pouring temperature of 725 °C for (10±0.5) min. Finally, the melting was cast into the horizontal steel mould. A sample for inductively coupled plasma atomic emission spectroscopy (ICP-AES) was taken directly after pouring of the casting was completed.

Table 1 Composition of commercial A357 alloys (mass fraction, %)

Si	Mg	Ti	Impurity				Al
			Fe	Cu	Zn	Total	
7.18	0.55	0.10	0.10	0.01	0.01	≤0.05	Bal.

Some samples of the castings were prepared for mechanical testing. The microstructure characterization of the samples was carried out by SEM (Apollo 300) operated at 25 kV. Phase identification was performed by a RIGAKU RINT-2000 X-ray diffractometer with Cu K_α radiation and an image plate detector over the 2θ range of 20°−90° at 0.02º step size. The tensile test was carried out by Instron 8801-50kN machine. For tensile testing, all of the samples were cut and polished into dog-bone-shaped specimens with a gauge length of 100 mm and a cross nummular section of d8.0 mm. The operation of the testing machine was computer-controlled and the digital data of load and displacement from the gage section were recorded. Tensile specimens were tested at an quasi-static strain rate of $5\times10^{-4}s^{-1}$, with direct measurement of the displacement of the tensile gage section by infrared ray.

3 Results and discussion

3.1 Microstructural characteristics

The most common ternary Al−5Ti−1B grain refiner used contains 5.0% Ti and 1.0% B (mass fraction). Al−Ti−B refiners consist of TiB_2 particles of 0.1−10 μm in diameter and Al_3Ti particles of 20−50 μm in diameter, dispersed in an aluminium matrix. Al_3Ti and TiB_2 can be

Table 2 Composition of Al−5Ti−1B and Al−5Ti−1B−RE grain refiners (mass fraction, %)

Master alloy	Ti	B	La	Ce	Fe	Si	Mn	Cr	Zr	Al
Al5Ti1B	4.93	0.98	−	−	0.20	0.06	<0.02	<0.02	<0.03	Bal.
Al5Ti1B1RE	4.99	1.13	0.28	0.74	0.18	0.06	<0.02	<0.02	<0.03	Bal.
Al5Ti1B2.0RE	5.00	1.06	0.37	1.61	0.19	0.06	<0.02	<0.02	<0.03	Bal.
Al5Ti1B3.0RE	4.96	1.10	0.60	2.24	0.18	0.06	<0.02	<0.02	<0.03	Bal.
Al5Ti1B4.0RE	5.14	1.00	0.36	3.86	0.31	0.06	<0.02	<0.02	<0.03	Bal.

very effective nucleants for aluminium. Such studies show that nucleation of α(Al) occurs on the basal faces of TiB_2 particles coated with Al_3Ti [22]. However, when the rare earth elements were added in A1−5Ti−1B grain refiner, the phases in this alloy were changed. XRD patterns of the Al−5Ti−1B−RE grain refiners with different RE compositions are shown in Fig. 1. It is found that the grain refiner with the RE composition of 2.0% consists of α(Al), $TiAl_3$, TiB_2 and $Ti_2Al_{20}RE$ (Fig. 1(a)), and $Ti_2Al_{20}RE$ phase occurs compared to the conventional ternary A1−5Ti−1B master alloy; with 3.0%, the grain refiner comprises of α(Al), TiB_2 and $Ti_2Al_{20}RE$ (Fig. 1(b)); with 4.0%, the grain refiner comprises of α(Al), TiB_2, $Ti_2Al_{20}RE$ and Al_4RE (Fig. 1(c)). According to Hall-Williamson equation which can calculate grain size and lattice strain of the Al matrix [23], with RE concentration increasing, the mean grain size of $TiAl_3$ particles in Al−Ti−B−RE decreases, while the mean grain size of $Ti_2Al_{20}RE$ particles increases.

Scanning electron microscopy (SEM) images of the A1−5Ti−1B−RE grain refines are shown in Fig. 2. It mainly contains α(Al) matrix and some irregular shaped particles (size of 50−60 μm) with bright shell and grey contrast core which is surrounded by the shell. With the RE composition of 2.0%, there exists mainly bulk $TiAl_3$ phase distributed in the α(Al) matrix, which are enwrapped in fine $Ti_2Al_{20}RE$ phases. The thickness of the shell increases with RE content increasing, while

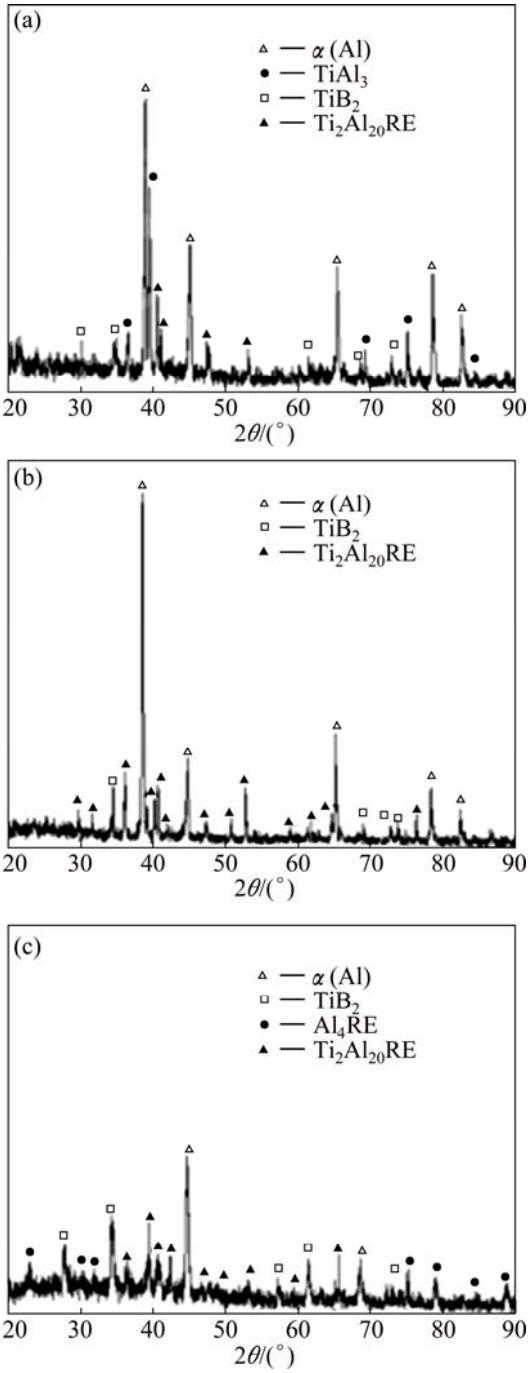

Fig. 1 XRD patterns of A1−5Ti−1B grain refiners with different RE compositions: (a) 2.0%; (b) 3.0%; (c) 4.0%

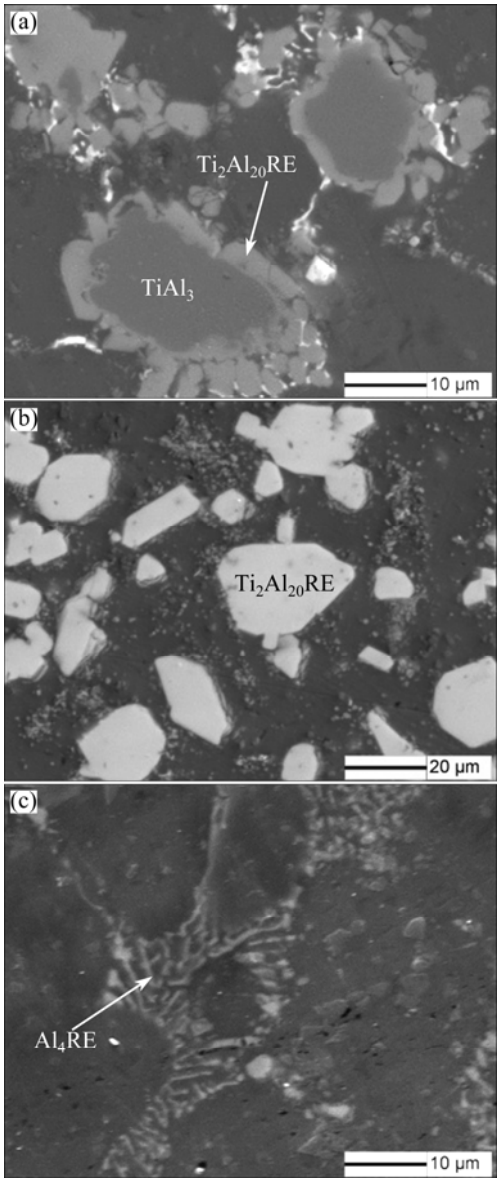

Fig. 2 SEM images of A1−5Ti−1B grain refiners with different RE compositions: (a) 2.0%; (b) 3.0%; (c) 4.0%

there is no significant change in size of the particles. The core-shell structure is decomposed with RE content increasing to 3.0%. $TiAl_3$ phase disappears and the bulk particles are only the finer $Ti_2Al_{20}RE$ phase. Some Al_4RE particles with grid structure are found with 4.0% RE.

The physical parameters of each phase in Al−Ti−B−RE grain refiner are shown in Table 3. From Table 3, it is found that TiB_2, AlB_2 and $TiAl_3$ have almost the same lattice constant with Al. $Ti_2Al_{20}RE$ structure is face-centered cubic, which is the same as Al. The crystal structure of TiB_2 and AlB_2 is also exactly the same. This can meet the requirements of refining agent. Through the thermodynamic analysis, it shows that nucleation energy is the smallest when nucleation relies on TiB_2. When addition of the RE is 2.0%, nucleation of $TiAl_3$ coated with $Ti_2Al_{20}RE$ phase occurs on the basal faces of TiB_2 particles of nanoscale; when the addition of RE is 3.0%, $TiAl_3$ is dissolved, and there is only TiB_2 particles coated with $Ti_2Al_{20}RE$ phase. In addition, $Ti_2Al_{20}RE$ phase has more crystal faces matching with Al, which makes aluminum alloy to be more refined.

Table 3 Physical parameter of each phase in Al−Ti−B−RE grain refiners

Sample	*a*/Å	*b*/Å	*c*/Å	Lattice types
Al	4.050	4.050	4.050	FCC
TiB_2	3.028	3.028	3.230	HCP
AlB_2	3.005	3.005	3.253	HCP
$TiAl_3$	3.846	3.846	8.594	FCC
$Ti_2Al_{20}RE$	14.707	14.707	14.707	FCC
Al_4RE	4.430	4.430	10.230	FCC

3.2 Mechanical properties

Figure 3 shows the ultimate tensile strength (σ_b) of A357 alloy with an addition of 0.2% Al−Ti−B−RE grain refiner, in which the RE was added at levels of 2.0%, 3.0% and 4.0%, respectively. The results show that, the values of σ_b reach 341 MPa, with an addition of 0.2% Al−5Ti−1B−2.0RE grain refiner in the A357 alloy. The optimal σ_b of 363 MPa was obtained with an addition of 0.2% Al−5Ti−1B−3.0RE grain refiner in the A357 alloy; with 0.2% Al−5Ti−1B−4.0RE grain refiner, the strength σ_b of the A357 alloy began to decline obviously to 335 MPa.

In Al−5Ti−1B−3.0RE grain refiner, $Ti_2Al_{20}RE$ phase was formed as a result of consecutive reaction between $TiAl_3$ and RE, by the way RE precipitated and reacted with elements at the grain boundary, all of these contributed to the refining effect of the Al−5Ti−1B−RE master alloy as well as the ultimate tensile strength. However, the occurrence of Al_4RE with grid structure would impede the refining effect of the grain refiner, and the decline of σ_b could be explained.

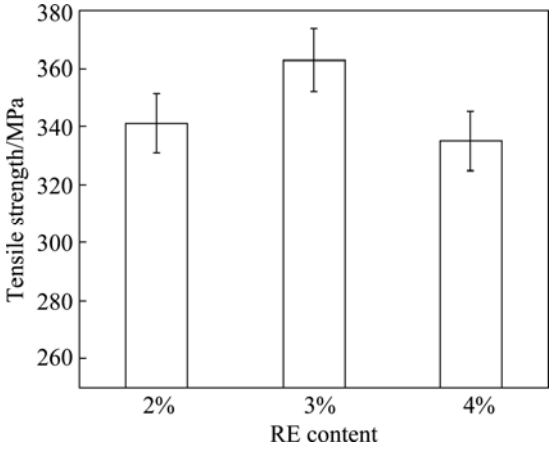

Fig. 3 Tensile strength of A357 refined with 0.2% Al−5Ti−1B−RE grain refiner with different RE contents

The tensile strength results show that σ_b of A357 with Al−5Ti−1B−3.0RE grain refiner reaches peak value. Thus, the effect of Al−5Ti−1B−3.0RE grain refiner on mechanical properties of A357 at different levels was discussed. In attempt to evaluate the mechanical properties of A357 with Al−5Ti−1B−3.0RE at different levels exactly, tensile tests were conducted at room temperature under uniaxial tensile loading, and the stress−strain curves are shown in Fig. 4. Contrasting with the A357 alloy, σ_b of A357 alloy with a level of 0.1% Al−5Ti−1B−3.0RE grain refiner increases obviously, the elongation of it decreases sharply. σ_b of refined A357 reaches peak value and the elongation recovers obviously at the level of 0.2%. With the level increasing, σ_b decreases apparently, but elongation almost has no change. The improved mechanical properties of the A357 alloy refined by adding the A1−5Ti−lB−3.0RE master alloy depend on the shape and size of α(Al) dendrites and eutectic silicon morphologies in the interdendritic region. The most significant improvement of tensile properties of the A357 alloy was obtained

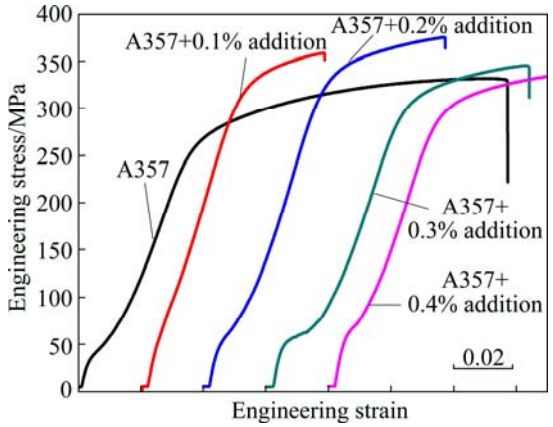

Fig. 4 Tensile strength variation of A357 alloy with different additions of Al−5Ti−1B−3.0RE grain refiner

at this concentration, due to the existence of the $Ti_2Al_{20}RE$ and TiB_2 phases, which can act as the heterogeneous nucleating sites, and σ_b can reach the maximum values of 363.5 MPa.

When the master alloys (i.e. Al−Ti, Al−B and A−Ti−B) are added to the aluminum melt, the aluminium matrix dissolves and then releases the intermetallic particles (i.e. $TiAl_3$, TiB_2, and $A1B_2$) into the melt to act as nucleates. $TiAl_3$ particles are believed to act as the heterogeneous nucleating sites in an A1−Ti binary alloy, and it is believed that in a ternary Al−Ti−B master alloy, TiB_2 particles act as the additional nucleating sites [22]. After the RE in the form of Al−5Ti−lB−3.0RE grain refiner are introduced into the A357 alloy, numerous potent smaller heterogeneous nuclei are dispersed in the melt, which promotes the nucleation of α(Al) grains. The grain refinement efficiency by introducing Ti, B and the rare earth elements is considerably better than that of adding Ti and B alone. TiB_2 and $Ti_2Al_{20}RE$ can act as the heterogeneous nucleating sites at this time. The TiB_2 particles in the refiner are faceted hexagonal platelets with large {0001} faces on which nucleation occurs. According to the nucleation theory, proposed by BRAMFITT, when misfit degree (δ) of some crystal nucleus and matrix is less than 6%, the nucleation is the most effective; when 6%<δ<15%, the effect on nucleation is medium; when δ>15%, the effect on nucleation declines obviously. $Ti_2Al_{20}RE$ phase has eight groups of matching relationship with Al phase, namely $Ti_2Al_{20}RE$ has better nucleation effect than $TiAl_3$. When the second phase $TiAl_3$ disappears, only $Ti_2Al_{20}RE$ and TiB_2 phases are left, which act as heterogeneous nucleation core, thereby improving the refining capacity. It is clearly seen that in the absence of grain refiner, the A357 alloy consisted of primary α(Al) dendrites and interdendritic needle/plate-like eutectic silicon distributing randomly (Fig. 5(a)). However, after adding the Al−5Ti−lB−3.0RE master alloy, the microstructures change from coarse dendrites to fine equiaxed α(Al) dendrites, and the eutectic silicon changes into tiny fibrous crystal from coarse acicular or flaky (Fig. 5(c)).

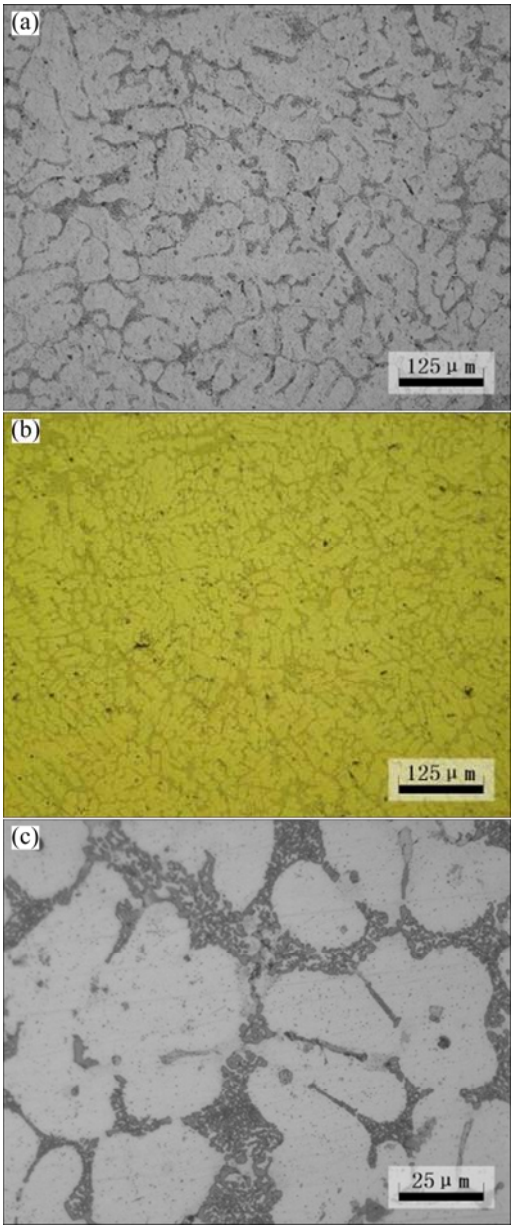

Fig. 5 OM images of A357 alloy before (a) and after (b, c) addition of Al−5Ti−1B−3.0RE

3.3 Tensile-fracture morphology

After tensile test, tensile fractured surfaces were observed by SEM to identify the fracture mode of the refined A357 alloy. Figure 6 shows the typical SEM images of the fracture morphologies of A357 alloy without and with adding 0.2% A1−5Ti−lB−3.0RE grain refiner. The fracture surface of the as-cast refined A357 alloy is mainly brittle in nature. The second phase holes can be clearly observed, which occur during the tension testing. As the addition level of the Al−5Ti−lB−3.0RE grain refiner increases, as shown in Fig. 6(b), the fractured surfaces of the refined A357 alloy exhibits fine, deep and uniformly distributed dimples, and there is about 45° between the fracture surface and the tensile direction. This information indicates that it belongs to ductile fracture mode. These phenomena indicate that fracture mode changes from brittle fracture to ductile fracture after the addition of Al−5Ti−lB−3.0RE grain refiner. It can be ascribed to the grain refinement of α(Al) grains, the distribution, and morphology improvement of silicon phase within the eutectic structures.

However, the distribution of particle diameters means that at any undercooling, only a fraction of the particles could ever be active growth centres. The exponential nature of the measured diameter distribution shows that a large fraction of the particles may never

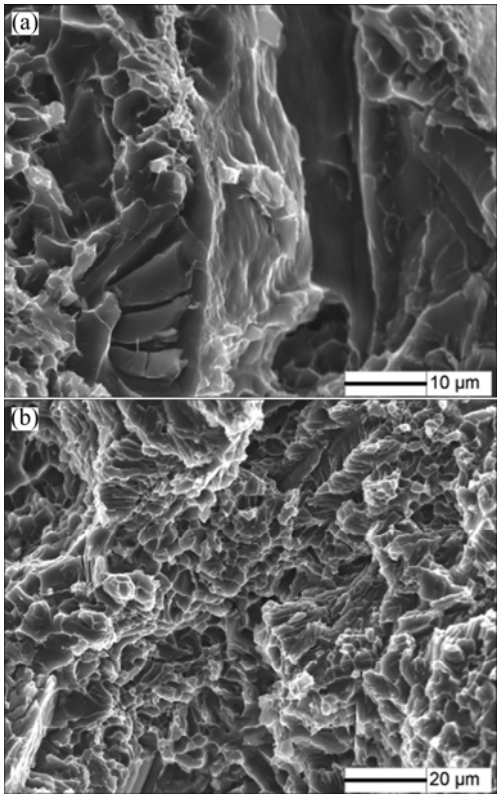

Fig. 6 Typical fracture morphology of A357 without (a) and with (b) adding 0.2% A1−5Ti−lB−3.0RE grain refiner

reach the undercooling at which they would become active [22]. So with the increasing addition of A1−5Ti−lB−3.0RE, an efficiency of 100% is impossible. Settling of inoculant particles is another reason in the experiment. These particles tend to settle at the bottom of crucibles resulting in the formation of sludge and reducing the overall efficiency of the refiner. Although settling appears to be negligible in the stirred melts used in the present experimental studies, this would not always be the case. Similarly, particle agglomeration may have to be taken into account for accurate modeling in some cases. As a result, all of these reasons contribute to the result that tensile strength and the elongation of A357 with 2% addition of Al−5Ti−1B−3.0RE grain refiner are appropriate.

4 Conclusions

1) By introducing the Al−5Ti−lB−3.0RE master alloy into A357, α(Al) matrix phase can be well refined from coarse dendrites to fine equiaxed dendrites, and the phase Si can be changed into tiny fibrous crystal from coarse acicular or layer.

2) Grain refinement is the key strengthening mechanism for the A357 alloy. The ultimate tensile strength of A357 alloy with Al−5Ti−1B−3.0RE grain refiner reaches the peak value of 363.5 MPa and the elongation recovers obviously at the same addition of grain refiner (0.2%).

3) The fracture mode of A357 alloy changes from brittle fracture to ductile fracture after the addition of Al−5Ti−lB−3.0RE grain refiner. This phenomenon indicates that there is an improvement on the ductility of this alloy.

References

[1] MUTRY B S, KORI S A, VENKATES W K, BHAT R R, CHAKRABORTY M. Manufacture of Al−Ti−B master alloys by the reaction of complex halide salts with molten aluminum [J]. Journal of Materials Processing Technology, 1999, 89−90: 152−158.

[2] YU Li-na, LIU Xiang-fa, WANG Zheng-qing, BIAN Xiu-fang. Grain refinement of A356 alloy by AlTiC/AlTiB master alloys [J]. Journal of Materials Science, 2005, 40(14): 3865−3867.

[3] VIOND KUMAR G S, MURTY B S, CHAKRABORTY M. Development of Al−Ti−C grain refiners and study of their grain refining efficiency on Al and Al−7Si alloy [J]. Journal of Alloys and Compounds, 2005, 396(1): 143−150.

[4] KORI S A, MURTY B S, CHAKRABORTY M. Development of an efficient grain refiner for Al−7Si alloy and its modification with strontium [J]. Materials Science and Engineering A, 2000, 283: 94−104.

[5] MOHANTY B S, GRUZLESKI J E. Mechanism of grain refinement in aluminium [J]. Acta Metallurgica et Materialia, 1995, 43(5): 2001−2012.

[6] MOHANTY B S, GRUZLESKI J E. Grain refinement mechanism of hypoeutectic Al−Si alloys [J]. Acta Materialia, 1996, 44(9): 3749−3760.

[7] ZHU Man, YANG Gen-cang, YAO Li-juan, CHENG Su-ling, ZHOU Yao-he. Influence of Al−Ti−B addition on the microstructure and mechanical properties of A356 alloys [J]. Rare Metals, 2009, 28(2): 181−186.

[8] AMBER L, BACKERUD L, KLANG H. Production and properties of master alloys of Al−Ti−B type and their ability to grain refine aluminium [J]. Metals Technology, 1982, 9(1): 1−6.

[9] MOHANTY P S, GUTHRIE R I L, GRUZLESKI J E. Studies on the fading behaviour of Al−Ti−B master alloys and grain refinement mechanism using LiMCA [C]//The 124th TMS Annual Meeting. Las Vegas, 1995: 859−868.

[10] YU Li-na, LIU Xiang-fa. The relationship between viscosity and refinement efficiency of pure aluminum by Al−Ti−B refiner [J]. Journal of Alloys and Compounds, 2006, 425: 245−250.

[11] LI Peng-ting, LI Yun-guo, NIE Jin-feng, LIU Xiang-fa. Influence of forming process on three-dimensional morphology of TiB_2 particles in Al−Ti−B alloys [J]. Transactions of Nonferrous Metals Society of China, 2012, 22(3): 564−570.

[12] CAO Fu-rong, WEN Jing-lin, DING Hua, WANG Zhao-dong, LI Ying-long, GUAN Ren-guo, HOU Hui. Force analysis and experimental study of pure aluminum and Al−5%Ti−1%B alloy continuous expansion extrusion forming process [J]. Transactions of Nonferrous Metals Society of China, 2013, 23(1): 201−207.

[13] HAN Guang, LIU Xiang-fa, DING Hai-min. Grain refinement of AZ31 magnesium alloy by new Al−Ti−C master alloys [J]. Transactions of Nonferrous Metals Society of China, 2009, 19(5): 1057−1064.

[14] CHEN Ya-jun, XU Qing-yan, HUANG Tian-you. Refining performance and long time efficiency of Al−Ti−B−RE master alloy [J]. The Chinese Journal of Nonferrous Metals, 2007, 17(8): 1232−1238. (in Chinese)

[15] QUESTED T E, GREER A L. The effect of the size distribution of inoculant particles on as-cast grain size in aluminium alloys [J]. Acta Materialia, 2004, 52(13): 3859−3868.
[16] BUNN A M, SCHUMACHER P, KEARNS M A, BOOTHYOYD C B, GREER A L. Grain refinement by Al−Ti−B alloys in aluminium melts: A study of the mechanisms of poisoning by zirconium [J]. Materials Science and Technology, 1999, 15(10): 1115−1123.
[17] GREER A L. Grain refinement of alloys by inoculation of melts [J]. Philosophical Transactions of the Royal Society of London. Series A: Mathematical, Physical and Engineering Sciences, 2003, 361(1804): 479−495.
[18] MCCARTNEY D G. Grain refining of aluminium and its alloys using inoculants [J]. International Materials Reviews, 1989, 34(1): 247−260.
[19] MURTY B S, KORI S A, CHAKRABORTY M. Grain refinement of aluminium and its alloys by heterogeneous nucleation and alloying [J]. International Materials Reviews, 2002, 47(1): 3−29.
[20] BASASAVAKUMAR K B, MUKUNDA R G, CHERTY M. Influence of grain refinement and modification on microstructures and mechanical properties of Al−7Si and A1−7Si−2.5Cu cast alloys [J]. Materials Characterization, 2008, 59(3): 283−289.
[21] FASOYINU F. Grain refinement of aluminum alloy 356 with scandium, zirconium, and a combination of titanium and boron [J]. Transactions of the American Foundry Society, 2001, 109: 1−21.
[22] GREER A L, BUNN A M, TRONCHE A. Modelling of inoculation of metallic melts: Application to grain refinement of aluminium by Al−Ti−B [J]. Acta Materialia, 2000, 48(11): 2823−2835.
[23] CULLITY B D, STOCK S R. Elements of X-ray diffraction [M]. 3rd. New York: Prentice-Hall 510 Inc, 2001.

Al−Ti−B−RE 细化剂对 Al−7.0Si−0.55Mg 合金显微组织和力学性能的影响

王雪姣[1]，徐 聪[1]，Arfan MUHAMMAD[1], Shuji HANADA[2]，
Hiroshi YAMAGATA[3]，王文红[4]，马朝利[1]

1. 北京航空航天大学 材料科学与工程学院，空天先进材料与服役教育部重点实验室，北京 100191；
2. Institute for Materials Research, Tohoku University, Sendai 980-8577, Japan；
3. Center for Advanced Die Engineering and Technology, Gifu University,
1-1 Yanagido, Gifu City, Gifu 501-1193, Japan；
4. 河北四通新型金属材料股份有限公司，保定 071105

摘 要：研究添加 Al−5Ti−1B−RE 细化剂对 Al−7.0Si−0.55Mg(A357)合金的显微组织和力学性能的影响。先利用真空熔炼技术制备 Al−7.0Si−0.55Mg 合金，然后在 Al−7.0Si−0.55Mg 合金中加入不同成分的 Al−5Ti−1B−RE 中间合金。通过 X 射线衍射仪(XRD)、金相显微镜(OM)和扫描电子显微镜(SEM)对显微组织和拉伸试样的断口形貌进行观察。在室温下对合金的力学性能进行测试。观察 Al−5Ti−1B−RE 细化剂的形态以及内部结构，可以发现以 TiB_2 为异质形核核心的 $TiAl_3/Ti_2Al_{20}RE$ 的壳层结构相。在 Al−7.0Si−0.55Mg 合金中加入 Al−5Ti−1B−3.0RE 细化剂后，抗拉强度会有明显提升，直到 0.2%添加量时，抗拉强度会达到峰值。

关键词：A357；Al−5Ti−1B 细化剂；稀土；断口；细化作用；抗拉强度

(Edited by Chao WANG)